JOURNAL OF MATERIALS SCIENCE 16 (1981) 1299–1304

Derivation of the tensile stress–strain curve from bending data

V. LAWS
Building Research Station, Building Research Establishment, Garston, Watford, UK

A method for calculating uniquely, the stress–strain curves in tension and compression from bending data, is described. The application of the method to cement-based composites is illustrated and the results compared with tensile curves measured directly.

List of symbols

σ stress
$\Delta\sigma$ increase in stress
σ_a apparent stress on the outer faces of a beam, calculated assuming a linear elastic beam in pure bending
ϵ strain
$\Delta\epsilon$ increase in strain
Y $\Delta\sigma/\Delta\epsilon$
F force
M moment
ΔM increase in moment
y distance from neutral axis in bending
d sample thickness
b sample width
c $d/(\epsilon_t - \epsilon_c)$
A area under tensile or compressive stress/strain curve
ΔA increase in area
Subscripts t and c refer to tension and compression respectively.

1. Introduction

Composites based on the reinforcement of a brittle material by glass or other fibres are usually non-linear in response to stress, and because of this show a response in bending apparently different from that in tension. Allen [1] and others have previously shown how the response in bending can be predicted from observed stress–strain curves in tension and compression; and Aveston *et al.* [2] have derived an analytical expression for the flexural strength in terms of the composition and properties of the components.

However, the bending curves predicted from measured tensile curves usually fall short of those measured directly, and in particular the apparent strain at failure in bending is often higher than that predicted. Laws and Ali [3] have shown that a stress capacity after failure in tension can lead to an increase in the strain at "failure" (i.e. at the maximum stress) in bending.

Laws and Walton [4] have outlined a method which uses data from a bending test to derive tensile stress–strain curves indirectly, for comparison with tensile curves measured directly. In this paper, the method is described in detail, and its application is discussed.

2. Theoretical details

Consider a rectangular beam of thickness d and width b, in pure bending under a bending moment M. The stress–strain relationships in tension and compression are described by the functions $\sigma_t(\epsilon)$ and $\sigma_c(\epsilon)$, respectively. Under pure bending, the longitudinal strains vary linearily with distance from the neutral axis, i.e.

$$y = c\epsilon, \qquad (1)$$

where y is the distance from the neutral axis, and c is a function of the outermost strains ϵ_t and ϵ_c:

$$c = d/(\epsilon_t - \epsilon_c). \qquad (2)$$

The convention that compressive stresses and strains are negative, is used.

It is assumed that plane sections remain plane; that the material is uniform in properties and that creep is negligible.

There are two conditions that apply, namely

(i) The total normal force acting on any crosssection is zero; i.e. the tensile forces are balanced by the compressive forces:

$$\sum F(y) = 0.$$

Using Equation 1 it follows that

$$bc\left[\int_{\epsilon_c}^{0} \sigma_c(\epsilon)\,d\epsilon + \int_{0}^{\epsilon_t} \sigma_t(\epsilon)\,d\epsilon\right] = 0, \quad (3)$$

and the areas A_t and A_c under the tensile and compressive stress–strain curves must be equal;

(ii) the total moment of the forces about the neutral axis is equal to the applied moment, M, i.e.

$$M = \sum F(y)y$$

$$= bc^2\left[\int_{\epsilon_c}^{0} \sigma_c(\epsilon)\,\epsilon\,d\epsilon + \int_{0}^{\epsilon_t} \sigma_t(\epsilon)\,\epsilon\,d\epsilon\right]. \quad (4)$$

Equations 3 and 4 allow two "unknowns" to be calculated.

2.1. Prediction of the bending curve from tensile data

To calculate the bending curve from tension and compression data, Equation 3 is used to find the strain on the compressive face for a given strain (and stress) on the tensile face. This locates the position of the neutral axis. The bending moment then follows from Equation 4.

The apparent stress on the outer faces of the beam, i.e. the stress that would apply if the beam were linearly elastic, is given by

$$\sigma_a = \frac{6M}{bd^2} \quad (5)$$

and is related to the bending moment by a numerical constant.

If the response in compression is linear, and the tensile curve can be represented by idealized "curves" the calculations are simple; and for stress–strain "curves" predicted by the ACK theory [5], analytical expressions can be written. However, where the curves in both tension and compression are non-linear the calculation of the strain on the compression face requires an iterative process; and the integrations are carried out numerically.

For the composites described later in this paper, it was assumed that the material was linear in compression with modulus equal to the initial modulus in tension. The location of the neutral axis is then simplified; but unless the equation for the tensile response is known, the calculation of the contribution of the tensile forces to the moment about the neutral axis, can only be performed numerically.

2.2. Deduction of the tensile and compression curves from bending

In Section 2.1, the stress–strain curves in tension and compression were "known", and Equations 3 and 4 were used to calculate the position of the neutral axis, and the bending moment. If the strains on the outer faces of the beam and the applied bending moment are known, it is equally valid to use Equations 3 and 4 to calculate the stress–strain curves in tension and compression. The method is not new [6], but does not appear to have been widely used.

It consists of the progressive calculation of the tensile and compressive stresses corresponding to the measured strain pairs as the bending moment increases. The progressively reconstructed tensile and compression stress–strain curves are used in the calculation of each subsequent tensile and compressive stress pair, as described in the Appendix.

The derivation of the stress pairs involves terms (see Equation A5 of the Appendix) that are extremely sensitive to the accuracy of strain measurement. However, each calculation depends on the previous ones; and an underestimate in one case will be "balanced" by an overestimate in the calculation of the next point. The result is that large fluctuation can occur in the stress pairs calculated as the strain is increased, particularly if the strain intervals chosen are small.

The procedure that has been adopted therefore is to "smooth" the calculated tensile and compressive stress–strain curves by a process of taking successive averages.

3. Application and discussion

Bending tests (four point) and tensile tests were carried out using Instron testing machines, models TTCM and 1115, respectively. Tensile tests were done at a constant rate of increase of strain; bending tests were carried out at a constant rate of cross-head travel, at a rate calculated to give a rate of strain increase approximately equal to that used in the tensile tests.

Fig. 1 shows results for an asbestos cement. Curves A and A′ show the apparent stress in bending, σ_a (Equation 5) as a function of the measured

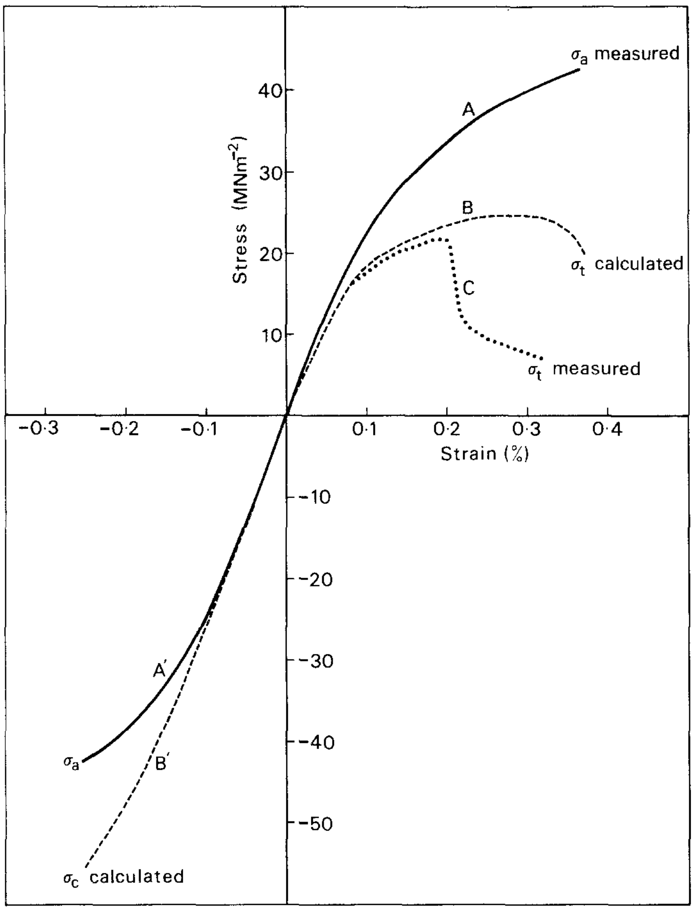

Figure 1 The apparent stress in bending as a function of measured strains on the tensile and compressive faces (curves A and A′, respectively) and the tension and compression curves (curves B and B′) deduced from the bending data. Curve C is a measured tensile curve for the same material (an asbestos cement).

strains; curves B and B′ show the tensile and compressive stress–strain curves deduced from that data. A measured tensile stress–strain curve for the same material is shown in C. The calculated and measured tensile stress–strain curves are similar, but that calculated from bending apparently continues to a higher strain.

The results for a grc composite containing 4.8% by weight of Cem-FIL* fibres 32 mm in length, and stored for 14 months in air at 40% RH and 20° C are shown in Fig. 2.

The strains were measured using an LVDT extensometer [7] which measured changes in linear length (chord). A correction was made to obtain changes in arc length (i.e. strains on the tensile and compression faces of the beam in bending). The strains achieved on both faces were high – over 1% on the tensile face and over 0.3% on the compression face. The tensile curve calculated from the bending data closely resembles that measured (in both tension and bending, three samples were tested and the results of each set were similar), except that it continues to a high strain (and stress). The calculated compression stress–strain curve is slightly non-linear up to approximately 60 MN m^{-2}; there is then an apparent stiffening, and at maximum (calculated) stress on the tensile face, the compression face supported a (calculated) stress of approximately 100 MN m^{-2} at a strain of about 0.3%.

The reason for this apparent change in slope of the compression stress–strain curve has yet to be explained. The compressive strength of grc is reported to be 60 to 100 MN m^{-2}, and it is possible, therefore, that failure occurs in compression, but leads to stiffening by obstruction of the "failed" region.

For wire-reinforced cements and mortars, some data [8, 9] taken from the literature has been analysed. Krenchel [8] measured the strains on the tensile and compressive faces of prisms in bending. The prisms consisted of mortar reinforced with a

*Trademark of Fibreglass Ltd, a Pilkington Bros subsidiary.

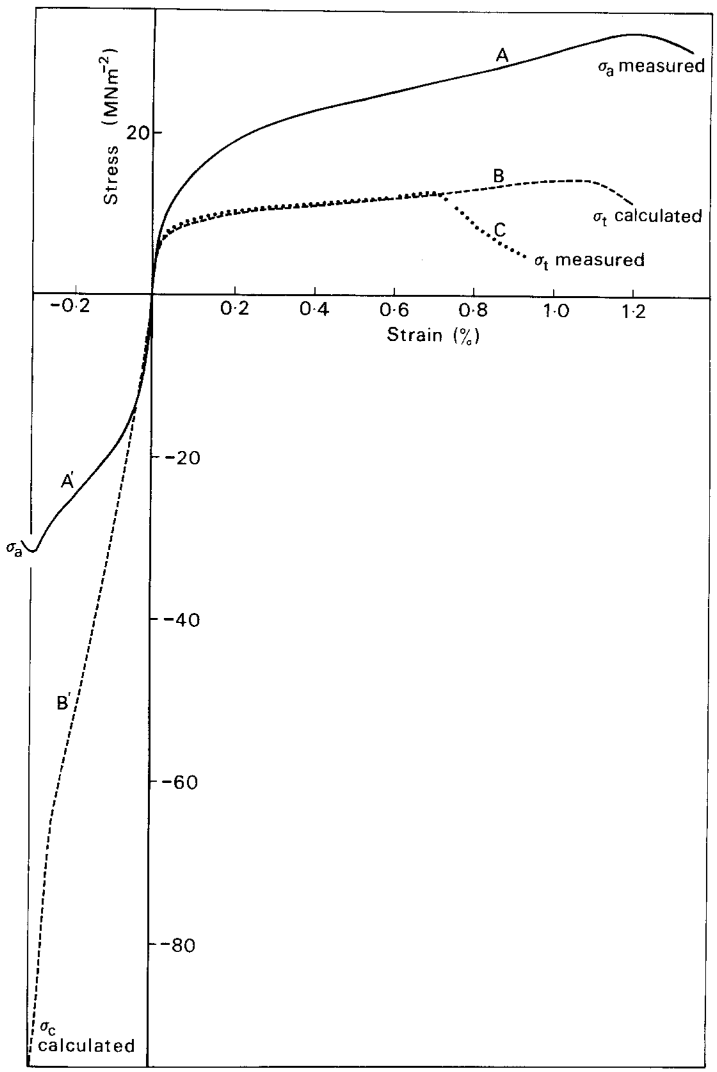

Figure 2 As Fig. 1 for a ductile grc.

2 vol% three-dimensional array of steel fibre, and the curve in bending rose continuously after the limit of proportionality, with no visible cracking before failure. Krenchel's data, together with the tension and compression curves deduced from the bending data are shown in Fig. 3. The deduced tensile curve shows a long "tail" beyond cracking, at a stress not very different from the cracking stress. This might imply some multiple cracking, assuming that this can occur at approximately constant stress. Analysis of Edgington's data [9] leads to deduced tensile stress–strain curves that show a long tail after "failure". Unfortunately there are no tensile stress–strain curves available with which to compare these deduced – the (direct) tensile curves measured by Edgington did not record any post failure stresses. However, Shah [10] reported the results of tests designed to measure the full stress–strain curves in tension of cement mortars reinforced with 1.73 vol% fibre. His results show slowly decreasing stress after failure implying single failure only. While there can be no strict comparison between the three sets of results since the composites were different, tensile curves deduced from Krenchel's [8] and Edgington's [9] data are generally in line with those observed by Shah [10].

4. Conclusions

A method has been described for calculating tensile and compressive curves from bending data. The method leads to unique results. The deduced tensile curves closely resemble those measured directly, except that they continue to higher

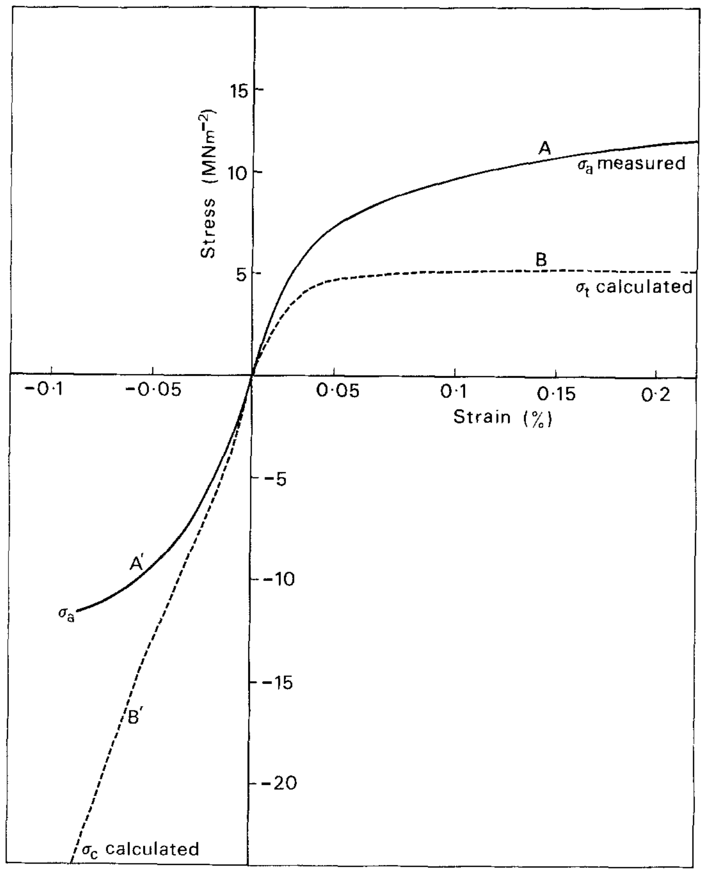

Figure 3 Wire-reinforced mortar, Data (A and A′) from [8] and tension and compression curves (B and B′) calculated from those data.

strains. The reason for this has yet to be investigated fully, but it could reflect a distribution of materials properties (a "size effect").

Further work is also needed to explain the shape of compression curve deduced in some cases, and in particular the apparent yield and stiffening at higher stresses. Work in both these areas is in progress.

Acknowledgements

I am grateful to Mr A. A. Langley and Mr P. L. Walton for providing the experimental data shown in Figs 1 and 2, respectively. The work described has been carried out as part of the research programme of the Building Research Establishment of the Department of the Environment and this paper is published by courtesy of the Director, Building Research Establishment, and by permission of the Controller HMSO, holder of Crown Copyright.

Appendix

(1) Suppose that under a measured bending moment M_0 sufficiently small that it can be assumed that both strains are below the elastic limit, the measured strains on the tensile and compressive faces are ϵ_{t0} and ϵ_{c0}, respectively. The stresses corresponding to these strains are σ_{t0} and σ_{c0}.

The balance of forces condition requires that the areas under the tension and compression stress–strain curves are equal, i.e. $A_{t0} = A_{c0}$, i.e.

$$\tfrac{1}{2}Y_{t0}\epsilon_{t0}^2 = \tfrac{1}{2}Y_{c0}\epsilon_{c0}^2$$

and

$$Y_{c0} = Y_{t0}(\epsilon_{t0}/\epsilon_{c0})^2, \qquad \text{(A1)}$$

where

$$Y_{t0} = \sigma_{t0}/\epsilon_{t0} \quad \text{and} \quad Y_{c0} = \sigma_{c0}/\epsilon_{c0}.$$

The second condition requires that the total moment of the forces $F(y)$ about the neutral axes equals the applied moment M_0,

$$M_0 = bc^2 \int_{\epsilon_{c0}}^{\epsilon_{t0}} \sigma(\epsilon)\,\epsilon\,\mathrm{d}\epsilon \qquad \text{(A2a)}$$

$$= \frac{bd^2}{(\epsilon_{t0} - \epsilon_{c0})^2}\,\tfrac{1}{3}(Y_{t0}\epsilon_{t0}^3 - Y_{c0}\epsilon_{c0}^3). \qquad \text{(A2)}$$

On substitution of Equation A1 into A2, Y_{t0} and hence σ_{t0} can be calculated. Y_{c0} and hence σ_{c0} then follow from Equation A1.

(2) Let the bending moment be increased by ΔM to M_1, and the measured strains by $\Delta\epsilon_t$ and $\Delta\epsilon_c$ to ϵ_{t1} and ϵ_{c1} respectively; the (unknown) stresses are σ_{t1} and σ_{c1}.

The analysis applies regardless of whether either or both these stresses are within or beyond the elastic limit/limits, and they may be greater or less than the previously calculated stresses. The only assumption made is that stress changes linearly with strain from σ_{t0} to σ_{t1} and σ_{c0} to σ_{c1} respectively. This is not an unreasonable assumption, particularly if the strain intervals used are small.

The balance of forces condition requires that the total areas under the tensile and compression stress–strain curves are equal. This reduces to

$$\Delta A_t = \Delta A_c \qquad \text{(A3)}$$

where ΔA_t and ΔA_c are the increases in area when the applied moment is increased by ΔM. Then, putting

$$Y_{t1} = (\sigma_{t1} - \sigma_{t0})/\Delta\epsilon_t$$

and

$$Y_{c1} = (\sigma_{c1} - \sigma_{c0})/\Delta\epsilon_c,$$

it follows that

$$\Delta\epsilon_t(\sigma_{t0} + \tfrac{1}{2}Y_{t1}\Delta\epsilon_t) = \Delta\epsilon_c(\sigma_{c0} + \tfrac{1}{2}Y_{c1}\Delta\epsilon_c)$$

from which

$$Y_{c1} = a_0 + a_1 Y_{t1} \qquad \text{(A4)}$$

where

$$a_0 = 2\Delta\epsilon_t\sigma_{t0}/(\Delta\epsilon_c)^2 - 2\sigma_{c0}/\Delta\epsilon_c$$

and

$$a_1 = (\Delta\epsilon_t/\Delta\epsilon_c)^2.$$

The total moment about the (new) neutral axis is

$$M_1 = bc^2\int_{\epsilon_{c1}}^{\epsilon_{t1}} \sigma(\epsilon)\,\epsilon\,\mathrm{d}\epsilon = \frac{bd^2}{(\epsilon_{t1}-\epsilon_{c1})^2}$$

$$\times\left[\int_{\epsilon_{c0}}^{\epsilon_{t0}} \sigma(\epsilon)\,\epsilon\,\mathrm{d}\epsilon + \int_{\epsilon_{c1}}^{\epsilon_{c0}} \sigma(\epsilon)\,\epsilon\,\mathrm{d}\epsilon + \int_{\epsilon_{t0}}^{\epsilon_{t1}} \sigma(\epsilon)\,\epsilon\,\mathrm{d}\epsilon\right].$$

The first integral in the above expression is from Equation A2a, equal to

$$\frac{M_0(\epsilon_{t0}-\epsilon_{c0})^2}{bd^2}.$$

It follows that

$$M_1 = a_2 + a_3 Y_{t1} + a_4 Y_{c1} \qquad \text{(A5)}$$

where

$$a_2 = \left(\frac{\epsilon_{t0}-\epsilon_{c0}}{\epsilon_{t1}-\epsilon_{c1}}\right)^2 M_0 + \frac{bd^2}{(\epsilon_{t1}-\epsilon_{c1})^2}$$

$$\times\,[\tfrac{1}{2}\sigma_{t0}(\epsilon_{t1}^2-\epsilon_{t0}^2) + \tfrac{1}{2}\sigma_{c0}(\epsilon_{c0}^2-\epsilon_{c1}^2)]$$

$$a_3 = \frac{bd^2}{(\epsilon_{t1}-\epsilon_{c1})^2}\,[\tfrac{1}{3}(\epsilon_{t1}^3-\epsilon_{t0}^3) - \tfrac{1}{2}\epsilon_{t0}(\epsilon_{t1}^2-\epsilon_{t0}^2)]$$

$$a_4 = \frac{bd^2}{(\epsilon_{t1}-\epsilon_{c1})^2}\,[\tfrac{1}{3}(\epsilon_{c0}^3-\epsilon_{c1}^3) - \tfrac{1}{2}\epsilon_{c0}(\epsilon_{c0}^2-\epsilon_{c1}^2)].$$

Equations A4 and A5 can then be solved for Y_{t1} and Y_{c1}, and hence for σ_{t1} and σ_{c1}.

(3) Successive stress pairs are calculated progressively in this way, using the previous information as it is accumulated (i.e. M_0, ϵ_{t0}, ϵ_{c0} in Equations A4 and A5 become M_1, ϵ_{t1}, ϵ_{c1}; M_1, ϵ_{t1}, ϵ_{c1} become M_2, ϵ_{t2}, ϵ_{c2}, and so on).

The calculation is easily carried out using a programmable calculator or computer and requires only a simple, straightforward program.

References

1. H. G. ALLEN, *J. Comp. Mater.* 5 (1971) 194.
2. J. AVESTON, R. A. MERCER and J. M. SILLWOOD, Composites – standard testing and design, Conference Proceedings, NPL, 8–9 April 1974 (IPC, London, 1974) p. 93.
3. V. LAWS and M. A. ALI, Fibre reinforced materials: Design and engineering applications, Conference Proceedings, Institution of Civil Engineers, London, March 1977 (ICE, London, 1977) p. 115.
4. V. LAWS and P. L. WALTON, RILEM Symposium, 1978, Testing and test methods of fibre cement composites (The Construction Press, Lancaster, 1978) p. 429.
5. J. AVESTON, G. A. COOPER and A. KELLY, The properties of fibre composites, Conference Proceedings, NPL, 4 November 1971 (IPC, London 1971) p. 15.
6. A. NADAI, "Plasticity", Engineering Societies Monographs (McGraw-Hill, New York and London, 1931) p. 165.
7. R. C. DE VEKEY, *J. Mater. Sci.* 9 (1974) 1898.
8. H. KRENCHEL, Structural Research Laboratory, Technical University of Denmark, Rapport Nr R42 (1973).
9. J. EDGINGTON, PhD thesis, University of Surrey (1974).
10. S. P. SHAH, RILEM Symposium, 1978, Testing and Test methods of fibre reinforced composites (The Construction Press, Lancaster, 1978) p. 399.

Received 6 October and accepted 10 November 1980.